

See discussions, stats, and author profiles for this publication at: <https://www.researchgate.net/publication/235644077>

Molecular Simulation Study on the Separation of Xylene Isomers in MIL-47 Metal–Organic Frameworks

ARTICLE *in* THE JOURNAL OF PHYSICAL CHEMISTRY C · DECEMBER 2009

Impact Factor: 4.77 · DOI: 10.1021/jp908247w

CITATIONS

37

READS

65

3 AUTHORS, INCLUDING:



J. M. Castillo

Universidad Pablo de Olavide

21 PUBLICATIONS 443 CITATIONS

SEE PROFILE



Sofia Calero

Universidad Pablo de Olavide

164 PUBLICATIONS 3,110 CITATIONS

SEE PROFILE

Molecular Simulation Study on the Separation of Xylene Isomers in MIL-47 Metal–Organic Frameworks

J. M. Castillo,^{†,‡} T. J. H. Vlugt,[‡] and Sofia Calero^{*,†}

Department of Physical, Chemical, and Natural Systems, University Pablo de Olavide, Ctra. de Utrera km. 1, 41013 Seville, Spain, and Delft University of Technology, Process & Energy Laboratory, Leeghwaterstraat 44, 2628CA Delft, The Netherlands

Received: August 26, 2009; Revised Manuscript Received: October 1, 2009

The separation performance of the metal–organic framework MIL-47 for xylene isomers was studied by Monte Carlo simulations in the grand-canonical ensemble. The experimental adsorption isotherms of xylene isomers in MIL-47 between 343 and 423 K were reproduced by using force fields available in the literature. Mixture isotherms were computed and compared with the mixture isotherms predicted by using pure component adsorption data and the ideal adsorption solution theory. This theory accurately predicts mixture isotherms of xylene isomers in MIL-47. The ideal adsorption solution theory was further employed to calculate the separation factors of xylene isomers in MIL-47. The order of preferential adsorption was found to be ortho > para > meta. The adsorption selectivity was found to increase with pressure, and the results showed a good agreement with the experimental data available. Henry coefficients and low coverage heats of adsorption and adsorption entropies were computed at 543 K showing an excellent agreement with experiments. It was found that the reason for adsorption selectivity is the interaction of CH₃ groups of neighboring molecules at high loadings, mainly for molecules adsorbed on the same wall of the MIL-47 channels.

1. Introduction

Xylene isomers are used commercially as organic solvents in the printing, rubber, and leather industries.¹ *p*-Xylene, the isomer with the largest industrial applications, is also used for the production of polyester, as the reactant (terephthalic acid) is obtained by oxidation of *p*-xylene.² *o*-Xylene is largely used in the production of phthalic anhydride, which is an additive used in the plastic industry.³ *m*-Xylene is a precursor of isophthalic acid, which is used as a copolymer in the synthesis of polyethylene terephthalate.⁴ To use the different xylene isomers for their particular industrial application, it is necessary to separate them. The separation of xylene isomers is not straightforward, as their physical properties are very similar. *o*-Xylene is the only isomer that can be separated via distillation due to their nearly identical boiling points (*o*-xylene: 144.5 °C; *m*-xylene: 139.3 °C; *p*-xylene: 138.5 °C at 1 atm⁵). Crystallization can be used for the separation of xylene isomers.^{6,7} However, the Parex process, based on adsorption in a simulated moving bed, is more frequently used for its larger production rate, better selectivity, and lower cost.⁸

The Parex process has been extensively studied to increase its performance. Reactors have been modified,^{9,10} and simulation methods have been employed¹¹ to optimize its productivity. The effects of different operation parameters, such as the surrounding equipment of the bed,¹² switching time,¹³ or the composition of the desorbents,¹⁴ have been extensively studied. The adsorbent used in this process is generally faujasite (FAU-type zeolite),¹¹ although other adsorbents such as cation-exchanged zeolite A (LTA-type zeolite) are also possible.¹⁵ Other types of materials have proved to be effective in the separation of xylene isomers,

such as silicalite,^{16,17} various polymers, and carbon materials^{18,19} or hydrotropes.²⁰ Recently, it was reported that the metal–organic materials MIL-47 and MIL-53 have large adsorption selectivity for xylene isomers.^{21–25}

Metal–organic frameworks (MOFs) are crystalline porous materials, composed by metal centers linked by organic molecules.²⁶ In general, this type of materials have the following properties: pores ranging from a few angstroms to 2–3 nm, low density, large surface areas, and a large potential for tailor-made design.²⁷ In its calcined form, MIL-47 consists of vanadium cations associated to six oxygen atoms, forming chains linked by terephthalic acid molecules. The porous structure of MIL-47 consists of 1-D, diamond-shaped straight channels (10.5 Å × 11.0 Å), where the metal centers lay at the vertices and the organic molecule on the walls of the channels. These channels are not interconnected. Framework flexibility in MIL-47 is not as important as that in MIL-53, another MOF with the same structure as MIL-47 but with a different metal center.²⁸

Modeling studies of MIL-47 are scarce. The adsorption properties of linear and branched alkanes and benzene in MIL-47 have been studied by molecular simulation.²⁹ The adsorption of carbon dioxide has been studied both by molecular simulation and by density functional theory calculations.³⁰ The self-diffusion coefficients of adsorbed molecules have only been computed for small molecules like methane³¹ and hydrogen.³² Simulation studies on the separation potential of this structure have been performed for nitrogen, methane, and carbon dioxide,³³ but we have not found any simulation study on xylene separation in MIL-47. Xylene adsorption has been extensively studied by molecular simulations in faujasite,^{34–36} and to a less extent in silicalite.³⁷

The objective of this work is to provide molecular insight on the separation mechanism for xylene isomers that takes place in MIL-47. For this purpose we will use molecular simulations

* To whom correspondence should be addressed. E-mail: scalero@upo.es.

[†] University Pablo de Olavide.

[‡] Delft University of Technology.

that will be compared with available experimental data. The result is that we are able to reproduce the experimentally pure component adsorption isotherms of xylene in MIL-47. The validity of the ideal adsorption solution theory is tested for predicting the adsorption isotherms of xylene mixtures in MIL-47. Finally, we study the arrangement of molecules in the MIL-47 pores at high loadings to understand the separation mechanism for xylene isomers that takes place in this material. The force field used in this work has been taken directly from force fields available in the literature. The remainder of this paper is organized as follows: in section 2 we present the simulation force fields and methods. We continue in section 3 with the results and discussion and in section 4 we present our conclusions.

2. Models and Simulation Details

Grand-canonical Monte Carlo (GCMC) simulations were used to compute the adsorption isotherms of xylene isomers and their mixtures at different temperatures. The Peng–Robinson equation of state³⁸ was used to relate pressures and fugacities or the pure components. The Lewis and Randall rule was used to calculate partial pressures of xylene mixtures in the gas phase.³⁹ The configurational-bias Monte Carlo technique⁴⁰ was used to efficiently insert and delete xylene molecules in the system. Henry coefficients, energies, enthalpies, and entropies of adsorption were computed from MC simulations in the NVT ensemble. Detailed information about the methodology can be found elsewhere.⁴¹ The MC simulations were performed in cycles and in each cycle one of the following trial moves was selected at random for each adsorbed molecule: translation, rotation, regrow at a random position, and insertion or deletion of a molecule (only for simulations in the grand-canonical ensemble). More details on the simulation technique can be found elsewhere.^{42,43} For calculating mixture isotherms, we also used trial moves that attempt to change the identity of an adsorbed molecule.⁴⁴ Xylene molecules tightly fit in the MIL-47 channels at high loadings. The acceptance probability of the insertion/deletion and identity change Monte Carlo moves is therefore small. For this reason, a large number of simulation cycles are needed both for equilibrating the system and for data production.

Xylenes were modeled with use of the OPLS force field for pure liquid substituted benzenes.⁴⁵ In this model, the carbon and hydrogen atoms forming part of the aromatic ring of the xylene molecules are described explicitly. The CH₃ groups are considered as single interaction centers. The interactions between xylene–xylene isomers and xylene–framework consist of Lennard-Jones and electrostatic interactions.

MIL-47 is modeled as a rigid structure. The crystal structure was obtained from the Cambridge Crystallographic Data Centre, file CCDC 632101-632101.⁴⁶ The Lennard-Jones dispersive interactions were taken from the DREIDING force field,⁴⁷ except those for the vanadium atoms which were taken from the UFF force field.⁴⁸ The use of a rigid framework is rationalized by the experimental observation that the presence of xylene molecules in MIL-47 does not alter the framework structure to a large extent.²¹ Rigid framework structures have been used in previous molecular simulation studies on adsorption and diffusion in MIL-47.^{29,31–33,49} It has been shown that the influence of framework flexibility on the computed adsorption isotherm in zeolites is negligible.⁵⁰ Therefore, it is reasonable to expect a similar behavior in other porous materials which do not exhibit a manifest

TABLE 1: Intermolecular Lennard-Jones Parameters and Partial Charges Used in This Work

| atom type | ϵ/k_B (K) | σ (Å) | q (e) |
|-----------------|--------------------|--------------|---------|
| MIL-47 | | | |
| V | 8.05 | 3.144 | 1.68 |
| O _a | 48.19 | 3.03 | −0.6 |
| O _b | 48.19 | 3.03 | −0.52 |
| C _a | 47.86 | 3.47 | −0.15 |
| C _b | 47.86 | 3.47 | 0.00 |
| C _c | 47.86 | 3.47 | 0.56 |
| H | 7.65 | 2.85 | 0.12 |
| xylene | | | |
| C | 35.24 | 3.55 | −0.115 |
| H | 15.03 | 2.42 | 0.115 |
| CH ₃ | 85.51 | 3.80 | 0.115 |

flexibility, as in the case of MIL-47. In the simulations, our system consisted of 16 unit cells of MIL-47 ($4 \times 2 \times 2$; $a = 6.1879$ Å, $b = 16.1430$ Å, $c = 13.9390$ Å). Each unit cell contains 72 atoms, of which 4 are vanadium, 20 oxygen, 16 hydrogen, and 32 carbon. The carbon and oxygen atoms of the structure are classified according to their bonding environment. C_a carbon atoms are bonded to one hydrogen and two other carbon atoms. C_b carbon atoms are bonded to another three carbon atoms. C_c carbon atoms are bonded to two oxygen atoms. O_a oxygen atoms are linked to two vanadium atoms and O_b to one vanadium and one carbon atom. The framework charges of MIL-47 were taken from the literature.²⁹

The Lennard-Jones interactions between different atoms of the system were obtained by using the Lorentz–Berthelot mixing rules. The Lennard-Jones potentials are truncated and shifted at a cutoff distance of 12 Å. Coulombic interactions were computed by using the Ewald summation with a relative precision of 10^{-6} . The parameters of the force field are given in Table 1.

3. Results and Discussion

The computed Henry coefficients, and heats of adsorption and entropy of adsorption at zero loading of xylene isomers in MIL-47 at 543 K are summarized in Table 2, together with experimental data.²³ The calculated Henry coefficients perfectly match the experimental data, having the same order of preferential adsorption (ortho > para > metha). The adsorption enthalpy of the xylene isomers in MIL-47 is identical within a deviation of less than 1%, revealing that the different isomers interact in a very similar way with the framework pores. The differences in adsorption entropy, although larger, are still too small to raise a definitive conclusion on the influence of steric effects in the adsorption. Nonetheless, the molecules with the lowest entropy of adsorption (in absolute value) are the most preferentially adsorbed.

The computed adsorption isotherms of pure *o*-, *m*-, and *p*-xylene at 343, 383, and 423 K are shown in Figures 1, 2, and 3 respectively, together with available experimental data.²³ At the highest temperature, the calculated isotherm is in very good agreement with the experiment. However, at the lowest temperature (343 K) the calculated isotherm overestimates the loading of *o*- and *p*-xylene, while at the higher temperatures (383 and 423 K) the loadings of *o*-xylene and *m*-xylene are underestimated at low pressures. One possible explanation for this discrepancy may be due to small changes in the framework structure with temperature. The adsorption of xylene molecules does not induce large changes

TABLE 2: Henry Coefficients, Heats of Adsorption, and Entropies of Adsorption at Zero Loading of Xylene Isomers in MIL-47 at 543 K^a

| molecule | K_H (mol/kg/Pa) | exptl | $-\Delta H$ (kJ/mol) | exptl | $-\Delta S$ (J/mol/K) |
|----------|--------------------------|----------------------|----------------------|---------|-----------------------|
| ortho | $2.70(3) \times 10^{-4}$ | 2.9×10^{-4} | 57.70(4) | 59.6(7) | 38.9(2) |
| meta | $1.89(2) \times 10^{-4}$ | 2.1×10^{-4} | 57.28(5) | 59.7(7) | 41.1(2) |
| para | $2.31(1) \times 10^{-4}$ | 2.2×10^{-4} | 57.70(2) | 61.2(4) | 40.2(1) |

^a The values in parentheses are the error in the last digit. Experimental values are also given for comparison.²³

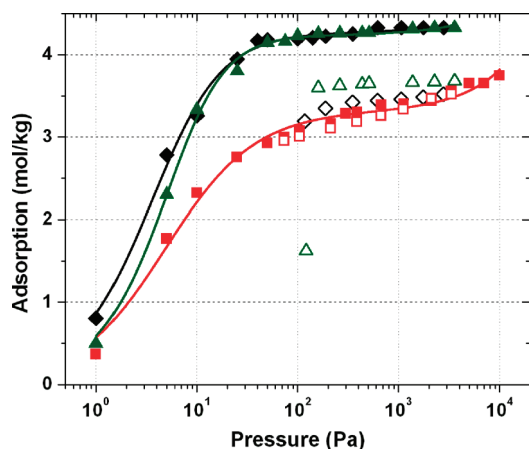


Figure 1. Adsorption isotherms of xylene in MIL-47 at 343 K: closed symbols, simulation data; open symbols, experimental data;²³ diamonds, *o*-xylene; squares, *m*-xylene; triangles, *p*-xylene; lines, fitting of the calculated isotherms using the Jensen equation (eq 1). Error bars are within the symbol size.

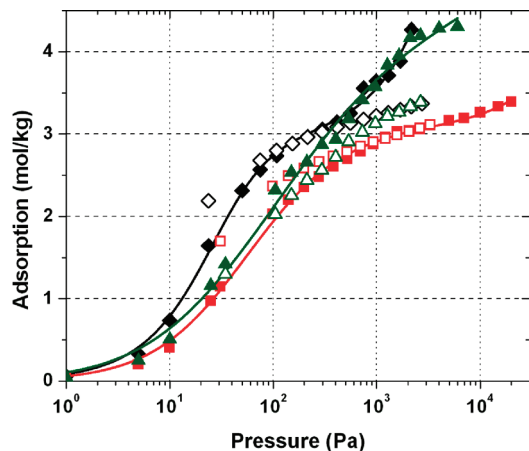


Figure 2. Adsorption isotherms of xylene in MIL-47 at 383 K: closed symbols, simulation data; open symbols, experimental data;²³ diamonds, *o*-xylene; squares, *m*-xylene; triangles, *p*-xylene; lines, fitting of the calculated isotherms using the Jensen equation (eq 1). Error bars are within the symbol size.

in the structure of MIL-47,²¹ although it has been shown that MIL-47 has some flexibility upon the adsorption of guest molecules, possibly sufficient to undergo changes in its crystal symmetry.⁵¹ The size of the rhombohedral channels of MIL-47 changes from 12.0×7.9 Å in the as-synthesized form to 11.0×10.5 Å after calcination.⁵² It is known that ethylbenzene and other organic molecules induce single crystal transformations in the structure.^{21,51} A comparison of experimental and simulation data suggest that at low temperatures, the xylene molecules induce a small contraction of the crystallographic structure, reducing the pore size of MIL-47 and therefore its adsorption capacity. Apparently, this effect is less pronounced for *m*-xylene. Note that the saturation

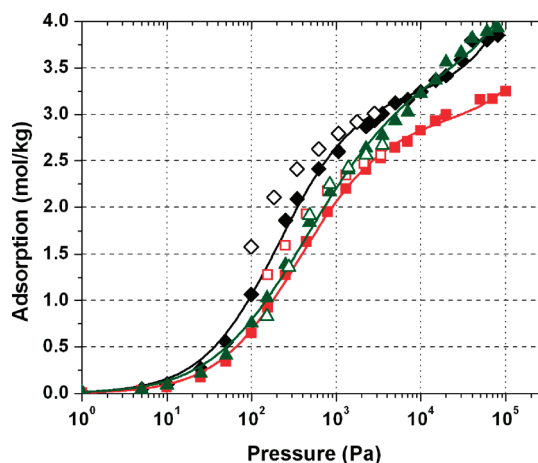


Figure 3. Adsorption isotherms of xylene in MIL-47 at 423 K: closed symbols, simulation data; open symbols, experimental data;²³ diamonds, *o*-xylene; squares, *m*-xylene; triangles, *p*-xylene; lines, fitting of the calculated isotherms using the Jensen equation (eq 1). Error bars are within the symbol size.

loading reached in our simulations was 4 molecules per unit cell (4.33 mol/kg), while experimentally the maximum loading reached was 3.4 molecules per unit cell.²³

The calculated isotherms were fitted by using the isotherm equation of Jensen,⁵³ also plotted as continuous lines in Figures 1–3:

$$n(P) = KP \left[1 + \left(\frac{KP}{a(1 + \kappa P)} \right)^c \right]^{1/c} \quad (1)$$

The pure component isotherms are well described with the Jensen isotherm, and their fitting parameters are given in Table 3. By using the fit to eq 1, the ideal adsorption solution theory⁵⁴ (IAST) was used to compute mixture isotherms from the pure component isotherms. The IAST was previously used successfully for calculating the mixture adsorption of carbon dioxide, nitrogen, and methane in MIL-47.³³ The mixture isotherms obtained from IAST were compared with the computed 50/50 binary mixtures of ortho–meta, ortho–para, and meta–para xylene, as well as with an equimolar, ternary mixture of *o*, *m*-, and *p*-xylene. These simulations were performed at 343, 383, and 423 K. As an example, in Figures 4 and 5 we show 50/50 mixture isotherms of *o*- and *m*-xylene, and a ternary mixture of xylenes respectively at 343 K. The agreement between the IAST and the calculated mixture isotherms was found to be acceptable for every system and temperature considered in this study. The IAST is therefore a recommendable method to calculate mixture isotherms in this system, as the computation of mixture isotherms of xylene in MIL-47 is very time-consuming and subject to large error bars. This is due to the large size of the xylene molecules that leads to a very low acceptance probability of the MC identity moves. Note that experimental measurement of these mixture isotherms can be challenging too, due to slow diffusion and the similarity of the molecules adsorbed.

TABLE 3: Fitting Parameters of the Jensen Equation (eq 1) for the Calculated Pure Component Adsorption Isotherms of *m*-, *o*-, and *p*-Xylene at 343, 383, and 423 K

| | <i>T</i> = 343 K | | | <i>T</i> = 383 K | | | <i>T</i> = 423 K | | |
|------------------------------|-----------------------|-----------------------|-----------------------|-----------------------|-----------------------|-----------------------|-----------------------|-----------------------|-----------------------|
| | ortho | meta | para | ortho | meta | para | ortho | meta | para |
| <i>K</i> (mol/kg/Pa) | 0.954 | 0.700 | 0.606 | 8.47×10^{-2} | 6.17×10^{-2} | 0.133 | 1.71×10^{-2} | 1.07×10^{-2} | 1.69×10^{-2} |
| <i>a</i> (mol/kg) | 4.269 | 3.314 | 4.239 | 2.968 | 3.109 | 4.777 | 3.257 | 2.984 | 3.655 |
| <i>κ</i> (Pa ⁻¹) | 7.53×10^{-6} | 1.53×10^{-5} | 8.09×10^{-6} | 2.02×10^{-4} | 5.23×10^{-6} | 4.32×10^{-6} | 2.87×10^{-6} | 1.11×10^{-6} | 1.84×10^{-6} |
| <i>c</i> (-) | 1.311 | 0.976 | 1.642 | 1.663 | 0.910 | 0.551 | 0.926 | 0.816 | 0.632 |

Our results for the selectivity are compiled in Table 4, calculated from the equimolar mixture isotherms obtained by the IAST. The selectivity is defined as:⁵⁵

$$S_{AB} = \frac{x_A y_B}{y_A x_B} \quad (2)$$

where *S* is the selectivity of component A relative to component B, *x_A* and *x_B* are the mole fractions of components A and B in the adsorbed phase, and *y_A* and *y_B* are the mole fractions of components A and B in the gas phase. If component A is preferentially adsorbed over B, *S_{AB}* is larger than 1, and vice versa. As can be seen from Figures 4 and 5, the selectivity was found to increase with pressure, reaching its maximum value

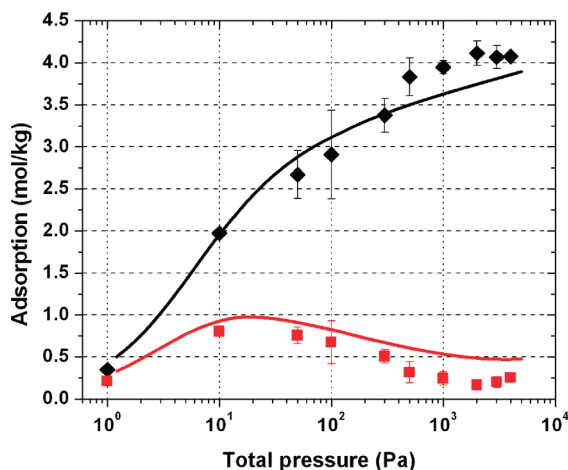


Figure 4. Calculated adsorption isotherm of a 50/50 binary gas mixture of *o*- and *m*-xylene in MIL-47 at 343 K: diamonds, *o*-xylene; squares, *m*-xylene; lines, mixture isotherm obtained with IAST.

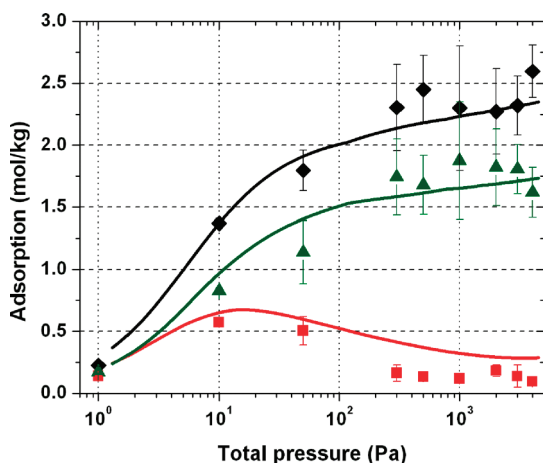


Figure 5. Calculated adsorption isotherm of an equimolar ternary gas mixture of *o*-, *m*-, and *p*-xylene in MIL-47 at 343 K: diamonds, *o*-xylene; squares, *m*-xylene; triangles, *p*-xylene; Lines, mixture isotherm obtained with IAST.

at saturation loading. This increase of selectivity with pressure agrees with previous experimental results.^{21,23}

The preferential order of adsorption is *o*-, *p*-, and *m*-xylene. This order is in agreement the computed Henry coefficients (Table 2) and with experimental selectivities obtained from batch adsorption, breakthrough curves, and zero coverage loading.^{21,23} At the temperatures considered here, the selectivities obtained at high loading are always significantly larger than the ones computed from the Henry coefficients. This indicates that the adsorption selectivity of xylene is caused by packing effects. Interestingly, the experimental para–meta selectivity is either larger or smaller than the ortho–meta depending on the method used to measure it.^{21–23} In our study, the ortho–meta selectivity is always larger than the para–meta selectivity. The same result is obtained experimentally when the selectivity is estimated by using zero coverage adsorption.²³ We speculate that this difference may be due to diffusion limitations in the experiments. The different selectivities increase with decreasing temperature, except for the ortho–para mixture that remains constant. For the equimolar ternary mixture, the calculated selectivities are the same as those for the binary mixture. Only in the case of the para–meta selectivity there is a small change in selectivity with respect to the binary mixture. The order of magnitude of the selectivities obtained is consistent with the experimental data available.^{21–23}

The selectivity of xylene isomers in MIL-47 has been attributed to packing effects.^{21,23} At high loadings it has been speculated that molecules are adsorbed by pairs, their benzene rings facing each other and approximately parallel to the aromatic rings of the terephthalic acid in the framework. The spatial arrangement of the CH₃ groups of every xylene opposing pair has been presented as the determining factor for preferential adsorption.^{21–23}

In Figure 6 we show snapshots of xylene molecules adsorbed in a MIL-47 channel along the *a* crystallographic direction. The snapshots were obtained from molecular simulations of pure component adsorption at high loading and 423 K. At these conditions, the benzene rings of the xylene molecules are approximately parallel to the aromatic rings of the framework structure. However, at lower loadings we find that the molecules have random orientations in the channel. Similar results have been obtained for benzene molecules adsorbed in MIL-47.²⁹ The difference with the interpretation of the experimental X-ray diffraction data is that at high loading the molecules are not adsorbed by pairs in the channel facing their aromatic rings. This configuration is not energetically favorable due to the electrostatic repulsion between the carbon and hydrogen atoms of facing aromatic rings. In our simulations, xylene molecules do not face the aromatic ring of other guest molecules on the opposite wall of the channel (face–face configuration), but instead the void spaces between them (face–side configuration, see Figure 6). This latter arrangement causes the distances between carbon atoms of one xylene molecule and the hydrogen atoms of the opposite xylene molecules in the channel to be

TABLE 4: Adsorption Selectivities of Xylene Mixtures in MIL-47 at 343, 383, and 423 K^a

| mixture | T = 343 K | | | | T = 383 K | | | | T = 423 K | | | |
|-----------------|------------|------------|------------|-------|-----------|-----|-----|-------|-----------|-----|-----|-------|
| | o-m | o-p | m-p | o-m-p | o-m | o-p | m-p | o-m-p | o-m | o-p | m-p | o-m-p |
| component 1 | o | o | p | o | o | o | p | o | o | o | p | o |
| component 2 | m | p | m | p | m | p | m | p | m | p | m | p |
| S _{om} | 8.2 (1.17) | | | 8.2 | 3.5 | | | 3.5 | 3.2 | | | 3.2 |
| S _{op} | | 1.4 (1.01) | | 1.4 | | 1.5 | | 1.5 | | 1.5 | | 1.5 |
| S _{pm} | | | 5.7 (2.07) | 6.0 | | | 3.0 | 2.3 | | | 1.9 | 2.1 |

^a Selectivities were calculated from eq 2 using the equimolar IAST mixture isotherms. The molar fraction of the components adsorbed was calculated from the adsorption at the largest pressure reached by the isotherm. o = *o*-xylene; m = *m*-xylene; p = *p*-xylene. Component 1 is the preferentially adsorbed isomer in the mixture, component 2 is the second. Experimental values obtained from breakthrough experiments are included in parentheses for comparison.²³

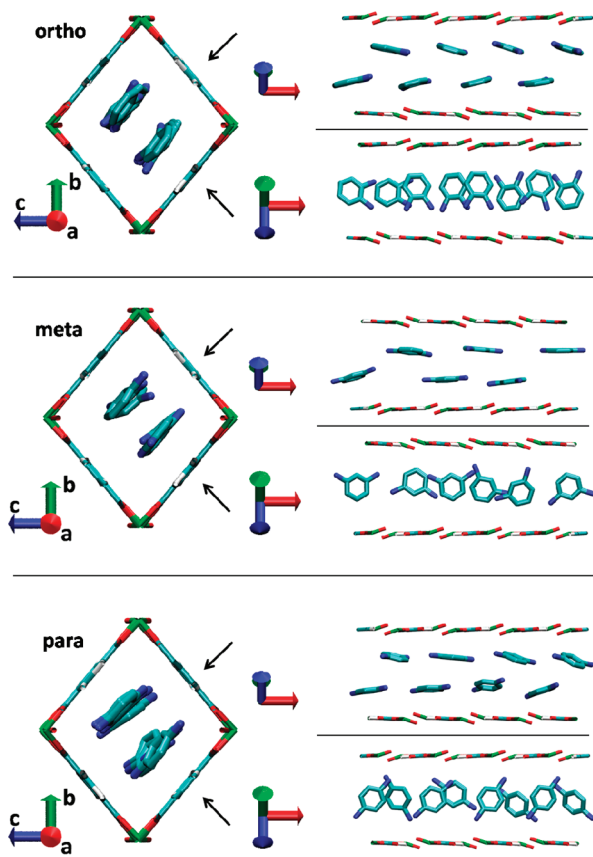


Figure 6. Snapshots of xylene molecules adsorbed in a single channel of MIL-47 at high loading (4 molecules per unit cell for ortho and para, and 3.5 molecules per unit cell for meta) and 343 K, obtained from molecular simulations. For the xylene molecules, the CH₃ groups are shown in dark blue, and their hydrogen atoms have been removed. On the right we show side views of the framework with part of the framework atoms removed for clarity. The orientation of the side views is indicated by the black arrows.

minimal, decreasing the electrostatic interaction energy. These two configurations have been previously reported for benzene dimers, the face–side configuration having lower energy.⁵⁶ In simulations of xylene in MIL-47 at low pressures we have also found T configurations, the lowest energy configuration for the benzene dimer,⁵⁶ as well as face–face configurations. The differences between the experimental and the simulation results may be due to the different temperature used in the experimental and simulation studies. The X-ray diffraction data were obtained at ambient temperature, while the lowest temperature studied by simulations was 343 K. It has been previously suggested that the molecular packing is slightly different at room temperature and at temperatures larger than 383 K.²³

At high loading, the aromatic rings of the *o*-xylene molecules adsorbed close to the same channel wall have the same orientation. The angle between the aromatic rings of *o*-xylene and the channel wall is around 25° (Figure 6). *o*-Xylene molecules adsorbed on opposite channel walls are close to a T arrangement. This arrangement increases the packing efficiency and reduces the interaction energy between adsorbed xylene molecules. *p*-Xylene molecules adsorbed on the same channel have the same orientation of their CH₃ groups. Therefore, the packing efficiency of *p*-xylene is caused by the arrangement of the CH₃ groups of the xylene molecules adsorbed on the same face of the channel, and to a less extent by the arrangement on the opposite channel wall. In the case of *m*-xylene, the disposition of the CH₃ groups of neighboring molecules does not allow either a favorable arrangement of the CH₃ groups or a T configuration of their aromatic rings. Therefore, the distance between *m*-xylene molecules is larger than that for the other two isomers and the saturation loading is only reached at higher pressures. This is in agreement with the computed pure component isotherms. We did not distinguish any appreciable different arrangement of molecules at different temperatures, as was previously suggested.²³

4. Conclusions

Both experiments and molecular simulations show a large adsorption selectivity of xylene isomers in MIL-47. Our simulations show that this selectivity is due to differences in the packing of xylene isomers. The ideal adsorption solution theory is a valuable tool to model the mixture adsorption of xylene isomers in MIL-47. The selectivity factors obtained at low temperatures are larger than the experimental ones (Table 4). This may suggest that the experimental selectivity of xylenes in MIL-47 can still be improved. In our simulations we use pure crystals, while real MIL-47 crystals may contain defects that may reduce their separation efficiency. In addition, the saturation loading found in the simulations might be difficult to achieve experimentally.

Acknowledgment. This work is supported by the Spanish “Ministerio de Educación y Ciencia (MEC)” (CTQ2007-63229), the Junta de Andalucía Excellence Project (P07-FQM-02595), the Eurosim project, and The Netherlands Organization for Scientific Research (NWO-CW) through the VIDI grant of T.J.H.V.

References and Notes

- (1) Flick, E. W. *Industrial solvents handbook*, 5th ed.; William Andrew: Weswood, NJ, 1999.
- (2) Scheirs, J.; Long, T. E. *Modern polyesters: chemistry and technology of polyesters and copolyesters*, 1st ed.; John Wiley & Sons, Ltd.: Chichester, UK, 2003.

- (3) Thorat, T. S.; Yadav, V. M.; Yadav, G. D. *Appl. Catal., A* **1992**, 90, 73.
- (4) Sakellarides, S. L. *Plast. Eng.* **1996**, 52, 33.
- (5) Hammond, P. D.; McArdle, E. H. *Ind. Eng. Chem.* **1943**, 35, 809.
- (6) Vicens, J.; Armah, A. E.; Fujii, S.; Tomita, K. I. *J. Inclusion Phenom. Mol. Recognit. Chem.* **1991**, 10, 159.
- (7) Shiau, L. D.; Wen, C. C.; Lin, B. S. *AIChE J.* **2008**, 54, 337.
- (8) Broughto, D. B.; Neuzil, R. W.; Pharis, J. M.; Brearley, C. S. *Chem. Eng. Prog.* **1970**, 66, 70.
- (9) Minceva, M.; Gomes, P. S.; Meshko, V.; Rodrigues, A. E. *Chem. Eng.* **2008**, 140, 305.
- (10) Jin, W. H.; Wankat, P. C. *Sep. Sci. Technol.* **2007**, 42, 669.
- (11) Kurup, A. S.; Hidajat, K.; Ray, A. K. *Ind. Eng. Chem. Res.* **2005**, 44, 5703.
- (12) Minceva, M.; Rodrigues, A. E. *Sep. Sci. Technol.* **2003**, 38, 1463.
- (13) Drechsel, B.; Hantsch, W.; Weber, K. *Chem. Tech.* **1991**, 43, 57.
- (14) Spindler, H.; Stief, C.; Hantsch, W.; Entner, R. *Chem. Tech.* **1990**, 42, 159.
- (15) Roethe, K. P.; Fiedler, K.; Roethe, A.; Suckow, M.; Stach, H.; Spindler, H.; Wittke, H.; Seidel, G.; Ermischer, W.; Roscher, W.; Seidel, R. *Chem. Tech.* **1985**, 37, 107.
- (16) Gu, X.; Dong, J.; Nenoff, T. M.; Ozokwelu, D. E. *J. Membr. Sci.* **2006**, 280, 624.
- (17) Guo, G. Q.; Chen, H.; Long, Y. C. *Microporous Mesoporous Mater.* **2000**, 39, 149.
- (18) Mohammadi, T.; Razaiean, M. P. *Sep. Sci. Technol.* **2009**, 44, 817.
- (19) Wu, X.; Yang, Y.; Tu, B.; Webley, P. A.; Zhao, D. *Adsorption* **2009**, 15, 123.
- (20) Ramesh, N.; Jayakumar, C.; Gandhi, N. N. *Chem. Eng. Technol.* **2009**, 32, 129.
- (21) Alaerts, L.; Kirschhock, C. E. A.; Maes, M.; van der Veen, M. A.; Finsy, V.; Depla, A.; Martens, J. A.; Baron, G. V.; Jacobs, P. A.; Denayer, J. E. M.; De Vos, D. E. *Angew. Chem., Int. Ed.* **2007**, 46, 4293.
- (22) Alaerts, L.; Maes, M.; Jacobs, P. A.; Denayer, J. E. M.; De Vos, D. E. *Phys. Chem. Chem. Phys.* **2008**, 10, 2979.
- (23) Finsy, V.; Verelst, H.; Alaerts, L.; De Vos, D. E.; Jacobs, P. A.; Baron, G. V.; Denayer, J. E. M. *J. Am. Chem. Soc.* **2008**, 130, 7110.
- (24) Finsy, V.; Kirschhock, C. E. A.; Vedts, G.; Maes, M.; Alaerts, L.; De Vos, D. E.; Baron, G. V.; Denayer, J. F. M. *Chem.—Eur. J.* **2009**, 15, 7724.
- (25) Krishna, R.; van Baten, J. M. *Mol. Simul.* **2009**, 35, 1098.
- (26) Batten, S. R. *Curr. Opin. Solid State Mater. Sci.* **2001**, 5, 107.
- (27) Chae, H. K.; Siberio-Perez, D. Y.; Kim, J.; Go, Y.; Eddaoudi, M.; Matzger, A. J.; O'Keeffe, M.; Yaghi, O. M. *Nature* **2004**, 427, 523.
- (28) Serre, C.; Millange, F.; Thouvenot, C.; Nogues, M.; Marsolier, G.; Louer, D.; Ferey, G. *J. Am. Chem. Soc.* **2002**, 124, 13519.
- (29) Finsy, V.; Calero, S.; Garcia-Perez, E.; Merklings, P. J.; Vedts, G.; De Vos, D. E.; Baron, G. V.; Denayer, J. F. M. *Phys. Chem. Chem. Phys.* **2009**, 11, 3515.
- (30) Ramsahye, N. A.; Maurin, G.; Bourrelly, S.; Llewellyn, P. L.; Serre, C.; Loiseau, T.; Devic, T.; Ferey, G. *J. Phys. Chem. C* **2008**, 112, 514.
- (31) Rosenbach, N.; Jobic, H.; Ghoufi, A.; Salles, F.; Maurin, G.; Bourrelly, S.; Llewellyn, P. L.; Devic, T.; Serre, C.; Ferey, G. *Angew. Chem., Int. Ed.* **2008**, 47, 6611.
- (32) Salles, F.; Jobic, H.; Maurin, G.; Koza, M. M.; Llewellyn, P. L.; Devic, T.; Serre, C.; Ferey, G. *Phys. Rev. Lett.* **2008**, 100, 245901.
- (33) Liu, B.; Smit, B. *Langmuir* **2009**, 25, 5918.
- (34) Beauvais, C.; Boutin, A.; Fuchs, A. H. *Adsorption* **2005**, 11, 279.
- (35) Moise, J. C.; Bellat, J. P. *J. Phys. Chem. B* **2005**, 109, 17239.
- (36) Lachet, V.; Boutin, A.; Tavittian, B.; Fuchs, A. H. *Langmuir* **1999**, 15, 8678.
- (37) Chempath, S.; Snurr, R. Q.; Low, J. J. *AIChE J.* **2004**, 50, 463.
- (38) Robinson, D. B.; Peng, D. Y.; Chung, S. Y. K. *Fluid Phase Equilib.* **1985**, 24, 25.
- (39) Kenneth, D. *The principles of chemical equilibrium*, 4th ed.; Cambridge University Press: Cambridge, UK, 1981.
- (40) Frenkel, D.; Smit, B. *Understanding Molecular Simulation*, 2nd ed.; Academic Press: London, UK, 2002.
- (41) Vlucht, T. J. H.; Garcia-Perez, E.; Dubbeldam, D.; Ban, S.; Calero, S. *J. Chem. Theory Comput.* **2008**, 4, 1107.
- (42) Calero, S.; Dubbeldam, D.; Krishna, R.; Smit, B.; Vlucht, T. J. H.; Denayer, J. F. M.; Martens, J. A.; Maesen, T. L. M. *J. Am. Chem. Soc.* **2004**, 126, 11377.
- (43) Vlucht, T. J. H.; Krishna, R.; Smit, B. *J. Phys. Chem. B* **1999**, 103, 1102.
- (44) Martin, M. G.; Siepmann, J. I. *J. Am. Chem. Soc.* **1997**, 119, 8921.
- (45) Jorgensen, W. L.; Nguyen, T. B. *J. Comput. Chem.* **1993**, 14, 195.
- (46) Cambridge Crystallographic Data Centre: www.ccdc.cam.ac.uk/data_request/cif.
- (47) Mayo, S. L.; Olafson, B. D.; Goddard, W. A. *J. Phys. Chem.* **1990**, 94, 8897.
- (48) Rappe, A. K.; Casewit, C. J.; Colwell, K. S.; Goddard, W. A.; Skiff, W. M. *J. Am. Chem. Soc.* **1992**, 114, 10024.
- (49) Ramsahye, N. A.; Maurin, G.; Bourrelly, S.; Llewellyn, P. L.; Devic, T.; Serre, C.; Loiseau, T.; Ferey, G. *Adsorption* **2007**, 13, 461.
- (50) Vlucht, T. J. H.; Schenk, M. *J. Phys. Chem. B* **2002**, 106, 12757.
- (51) Wang, X.; Liu, L.; Jacobson, A. J. *Angew. Chem., Int. Ed.* **2006**, 45, 6499.
- (52) Barthelet, K.; Marrot, J.; Riou, D.; Ferey, G. *Angew. Chem., Int. Ed.* **2002**, 41, 281.
- (53) Jensen, C. R. C.; Seaton, N. A. *Langmuir* **1996**, 12, 2866.
- (54) Myers, A. L.; Prausnitz, J. M. *AIChE J.* **1965**, 11, 121.
- (55) Krishna, R.; Smit, B.; Calero, S. *Chem. Soc. Rev.* **2002**, 31, 185.
- (56) Jorgensen, W. L.; Severance, D. L. *J. Am. Chem. Soc.* **1990**, 112, 4768.

JP908247W